Turbulent heat transfer in a flat plate boundary layer disturbed by a cylinder

E. Marumo*, K. Suzuki† and T. Sato‡

Augmentation of heat transfer from a flat plate using a turbulence promoter has been studied. A circular cylinder 8 mm in diameter was placed in the turbulent boundary layer detached from the flat plate. It was located parallel to the plate and perpendicular to the flow direction. Clearance, c, between the cylinder and the flat plate was varied in nine steps: c=0, 1, 2, 3, 4, 6, 11, 20 and 29.5 mm. Measurements were made of the local heat transfer coefficients, mean velocity profiles, turbulence intensity profiles, static pressure and skin friction. Experimental results showed that the heat transfer deterioration which occurs just downstream of the cylinder at c=0 mm can be removed by displacing the cylinder a small distance from the wall. The improvement in heat transfer is mainly due to the unsteadiness of the recirculating flow on the plate and the effect of intense turbulence arriving at the near wall region from the lower shear layer of the cylinder wake. Heat transfer augmentation is most effective when c=4 mm and becomes less effective when c is increased more than 6 mm. The enhancement disappears far downstream from the cylinder.

Keywords: *convective heat transfer, turbulence promoter, complex turbulent flow, relaxing turbulent flow*

Heat transfer augmentation is of practical importance from the viewpoint of effective use of thermal energy. This paper presents an investigation of a basic situation: the enhancement of turbulent heat transfer from a flat plate. A common method for enhancing heat transfer from a flat plate is to roughen the plate's surface or to place ribs on the surface. However, if a separation bubble attaches to the back of each rib it creates a region where wall heat transfer deteriorates. Thus, it is important to investigate whether more effective heat transfer augmentation is obtained when an obstacle corresponding to a rib is detached from the plate. Free stream turbulence also influences heat transfer enhancement. There are many studies of this effect, including the recent data of Simonich and Bradshaw[1]. The case studied here is that in which an obstacle generating turbulence is located close to, but detached from, the flat plate.

In this study, a turbulent boundary layer is disturbed by a single cylinder located in a two-dimensional geometrical position, ie normal to the flow direction and parallel to the flat plate. The mean flow and turbulence characteristics of this disturbed boundary layer have been studied previously both from statistical and structural viewpoints[2-6]. The case when an in-line array of cylinders is inserted into the boundary layer will be discussed in a later paper[7]. A similar heat transfer experiment was performed by Fujita *et al*[8]. The present paper gives a more detailed discussion of the mechanism of heat transfer augmentation using the mean flow and turbulence characteristics of the flow.

* Department of Mechanical Engineering, Akashi Technological College, Akashi, Hyogo, Japan
† Department of Mechanical Engineering, Kyoto University, Kyoto, Japan
‡ Department of Mechanical Engineering, Setsunan University, Osaka, Japan
Received 27 September 1984 and accepted for publication in final form on 24 April 1985

Experimental apparatus and procedures

A schematic view of the wind tunnel used in the present study, of cross section 380 mm × 380 mm, is shown in Fig 1. The leading edge of the flat plate is located 1500 mm downstream from the end of the 9:1 contraction nozzle. The flat plate is held at a distance of 45 mm from the floor of the wind tunnel, and the boundary layer developed on the floor upstream of the plate is sucked from the plate by an auxiliary blower. Two-dimensionality and uniformity of the flow at the leading edge were carefully established by adjusting the rate at which air was sucked off. Streamwise variations of the static pressure were minimized by attaching a plate to the tunnel's ceiling. Its thickness was machined so as to cancel the flow acceleration caused by the thickening of the boundary layer developing on the tunnel walls. The magnitude of pressure non-uniformity was kept within $\pm 0.3\%$ of the main stream dynamic pressure except for an inevitable abrupt pressure change which occurred at the streamwise position where the cylinder was placed.

The flat plate used in the present study is shown in Fig 2. The first 400 mm of the plate downstream of the leading edge was covered by sandpaper to trip the boundary layer. Heating of the surface started at the location 540 mm downstream from the leading edge. Seven strips of thin metal sheets 52 mm wide were glued on the surface of the flat plate. The spanwise space between two neighbouring strips was 1 mm. These strips were electrically connected in series and were heated by

 0142-727X/85/040241-08$3.00

passing an alternating electric current through them. Eighty-five thermocouples of 0.1 mm diameter were attached to the back surface of the middle metal strip in order to measure the streamwise distribution of surface temperature T_w. Twenty-two thermocouples were also attached to the back surface of the plywood plate. The temperature difference across the plywood, with the assumption of one-dimensional heat conduction, was used to evaluate the rate of heat conduction through the back surface of the plate. This heat loss was less than 5% of the uncorrected wall heat flux. The two-dimensionality of the thermal field was also checked and found to be satisfactory. Radiative heat loss from the plate to the tunnel wall was sufficiently small. The possibility of conductive heat loss to the cylinder occurring when the cylinder was attached to the plate was also small because

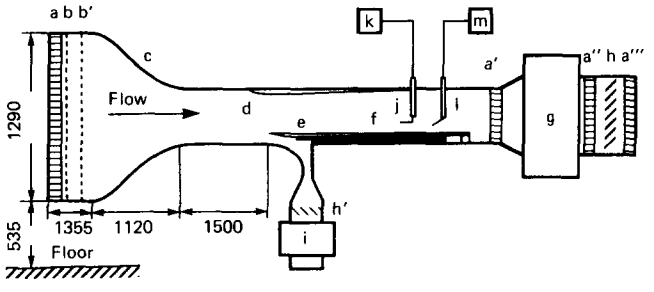

Fig 1 Wind tunnel: (a, a', a'', a''') honeycomb straightners; (b, b') stainless wire screens; (c) contraction chamber; (d) pressure adjustment plate; (e) test plate; (f) circular cylinder; (g) main blower; (h, h') flow controller; (i) suction blower; (j) separate Pitot-static tube; (k) inclined tube manometer; (l) hot wire probe; (m) constant temperature anemometer

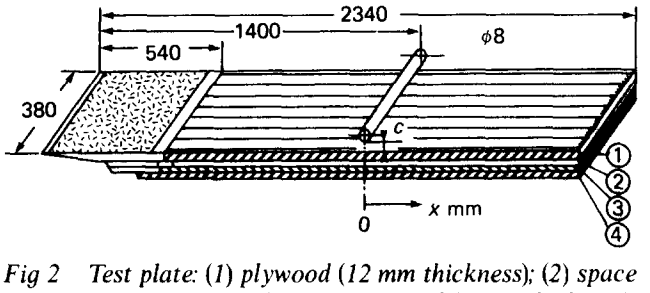

Fig 2 Test plate: (1) plywood (12 mm thickness); (2) space with air (4 mm thickness); (3, 4) plywood (9 mm thickness)

of the small contact area and the low thermal conductivity of the cylinder material. Measurements of the heat transfer coefficient for the case when no cylinder was inserted in the flat plate boundary layer were found to agree with an empirical equation given by Colburn[9]. All the experiments were carried out for a heating condition of uncorrected wall heat flux of 1 kW/m^2. The local heat transfer coefficient is defined as follows:

$$h_x = \frac{q_w}{T_w - T_\infty} \tag{1}$$

where q_w is the corrected wall heat flux. The main stream temperature T_∞ was measured with a thermocouple at the inlet to the wind tunnel.

A synthetic resin cylinder of 8 mm diameter was located at a streamwise position of 1400 mm downstream from the flat plate leading edge. It was held in a position normal to the flow direction and parallel to the flat plate. The space between the cylinder and the plate was changed in 9 steps: $c = 0$, 1, 2, 3, 4, 6, 11, 20 and 29.5 mm ($c/d = 0$, 0.13, 0.25, 0.38, 0.5, 0.75, 1.38, 2.5 and 3.69). Detailed experimental measurements of flow and turbulence characteristics have been made previously[2-6] for the three cases of $c = 2$, 11 and 29.5 mm. Additional experiments were performed in the unheated condition to obtain the mean velocity, intensity of streamwise velocity fluctuation, wall static pressure and wall shear stress. The first two data sets were obtained using a hot-wire anemometer. The hot wire probe was constructed using a 5 μm tungsten wire with copper plated ends having an effective length of 1 mm. The static pressure on the plate's surface and wall shear stress were measured separately using another acrylic flat plate with pressure detection holes of 0.3 mm diameter. The wall shear stress was obtained using a Preston tube which was constructed from a stainless steel tube of 1.25 mm outer diameter. Patel's calibration curve[10] was used to evaluate the magnitude of the wall shear stress. The present experimental data for the heat transfer, flow and turbulence characteristics are used together with previously reported data[2-6] in the discussion which follows.

Hot-wire measurement is not accurate either in recirculatory flows or in highly turbulent flows. Patel's calibration curve is valid only for the case when the logarithmic law of the wall exists near the wall. Thus,

Notation

- c Clearance between cylinder and plate, mm
- C_f Skin friction coefficient
- C_p Static pressure coefficient
- d Cylinder diameter, mm
- F_x Normalized average heat transfer coefficient
- h_x Local heat transfer coefficient, kW/m^{2}K
- p Static pressure, Pa
- p_∞ Main-stream static pressure downstream of cylinder, Pa
- q_w Wall heat flux, kW/m^2
- R_{uu} Auto-correlation of u
- T Temperature, K
- U Mean velocity parallel to main flow direction, m/s
- U_∞ Main stream velocity, 14 m/s
- u, u' Fluctuating component of streamwise velocity and its intensity, m/s
- x Streamwise distance from cylinder, mm
- x_{max} Position of the second h_x peak, mm
- y Distance from wall, mm
- α, β Constants in Eq (5)
- ρ Density of air, kg/m^3
- τ Time interval, ms

Subscripts

- 0 Undisturbed case
- w Wall
- ∞ Main stream

some of the data presently obtained with these methods are of low accuracy. These parts of the data will be shown by dotted lines in the figures which follow. In the discussion of the heat transfer mechanism, however, the knowledge about the flow near the wall is important especially when the recirculating flow appears near the wall. Therefore, flow visualization was additionally performed to confirm some of the inferences obtained through the above-mentioned measurements of low accuracy. In this experiment, three methods were applied: surface oil flow method, tuft method and fine particle method. In the last method, fine dried-up salt particles were spread over the flat plate.

Results and discussion

Experimental results

Streamwise distributions of the local heat transfer coefficient, h_x, obtained in the present experiments are shown in Figs 3(a) to 3(c) for several cases of different clearance between the cylinder and the plate. In these figures, the value of h_x is normalized with h_{x0}, the local heat transfer coefficient measured for a turbulent boundary layer undisturbed by a cylinder, and the abscissa x is the streamwise distance downstream from the position where the cylinder was inserted. The heat transfer from the flat plate is found to be augmented by the insertion of the cylinder into the flat plate boundary layer. The local heat transfer coefficient attains almost twice the value of h_{x0} at some streamwise locations when $c=4$ or

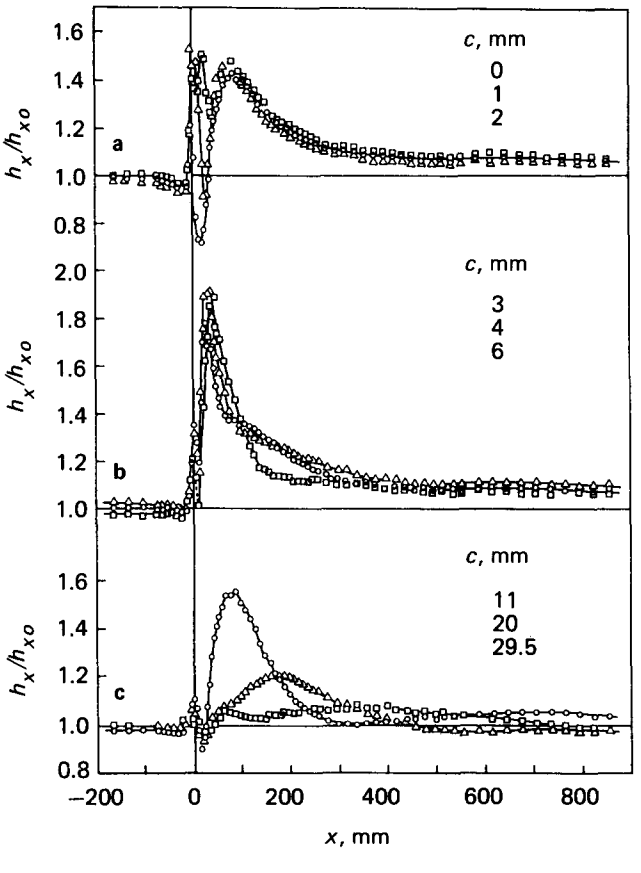

Fig 3 Normalized local heat transfer coefficients: (a) c = 0, 1, 2 mm; (b) c = 3, 4, 6 mm; (c) c = 11, 20, 29.5 mm

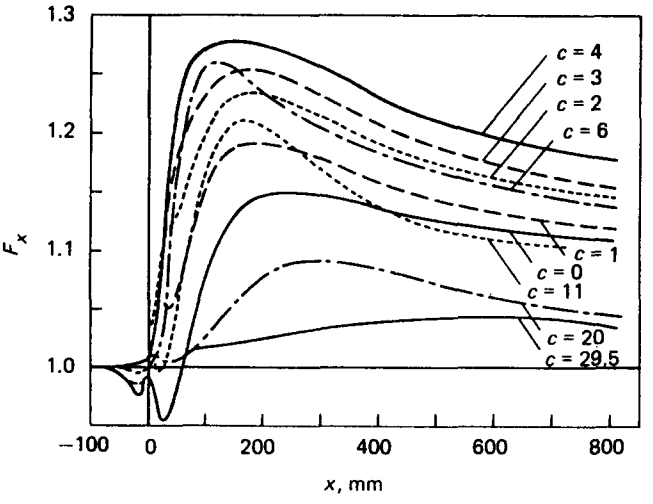

Fig 4 Normalized average heat transfer coefficient

6 mm ($c/d=0.5$ or 0.75). Except for the two largest cases of c, heat transfer is enhanced by more than 20% on average over the streamwise location from $0 \leqslant x \leqslant 300$ mm. This can be confirmed in Fig 4, which shows the ratio between the two averaged heat transfer coefficients $\overline{h_x}$ and h_{x0} as defined by:

$$F_x = \frac{\overline{h_x}}{h_{x0}} = \frac{\int_{-100}^{x} h_x \, dx}{\int_{-100}^{x} h_{x0} \, dx} \tag{2}$$

where x is measured in mm. Incidentally, almost the same magnitude of heat transfer enchancement was reported by Simonich and Bradshaw[1] for the case with increased level of free stream turbulence. However, the present study implies that higher heat transfer augmentation can be attained when multiple cylinders are located in an array with a pitch smaller than 300 mm. This case will be discussed in the companion paper[7]. The physical reason for the heat transfer augmentation found may be quite complex because the distributions of h_x vary not only quantitatively but also in shape with the change of c.

For use in later discussions of the h_x distributions, some results from the hydrodynamic experiments are presented here. Figs 5(a) to 5(d) show the transverse distributions of the average velocity U and of the intensity of the streamwise velocity fluctuation u'. As will be discussed later, a separation bubble extends to a position of $x \cong 80$ mm when $c=0$. Therefore, the results plotted in Fig 5(a) are assumed to be inaccurate at the streamwise locations within the range of $0 \leqslant x \leqslant 80$ mm, especially at transverse locations situated within the separation bubble. Positive values of U measured at such positions resulted from the inability of the hot-wire anemometer to detect flow direction. This must be kept in mind in later discussions.

Figs 6(a) to 6(c) show the streamwise distributions of the skin friction coefficient, C_f, for differenct values of clearance, c. All the data plotted in these figures were obtained with the Preston tube facing upstream. Supplementary experiments were performed directing the Preston tube downstream at those positions where negative values of C_f were observed in Fig 6(a). These data were found to agree qualitatively with the corresponding results shown in Fig 6(a) but slightly differ quantitatively. This is not unexpected since the Preston tube is believed to be accurate only when the flow is almost parallel to the

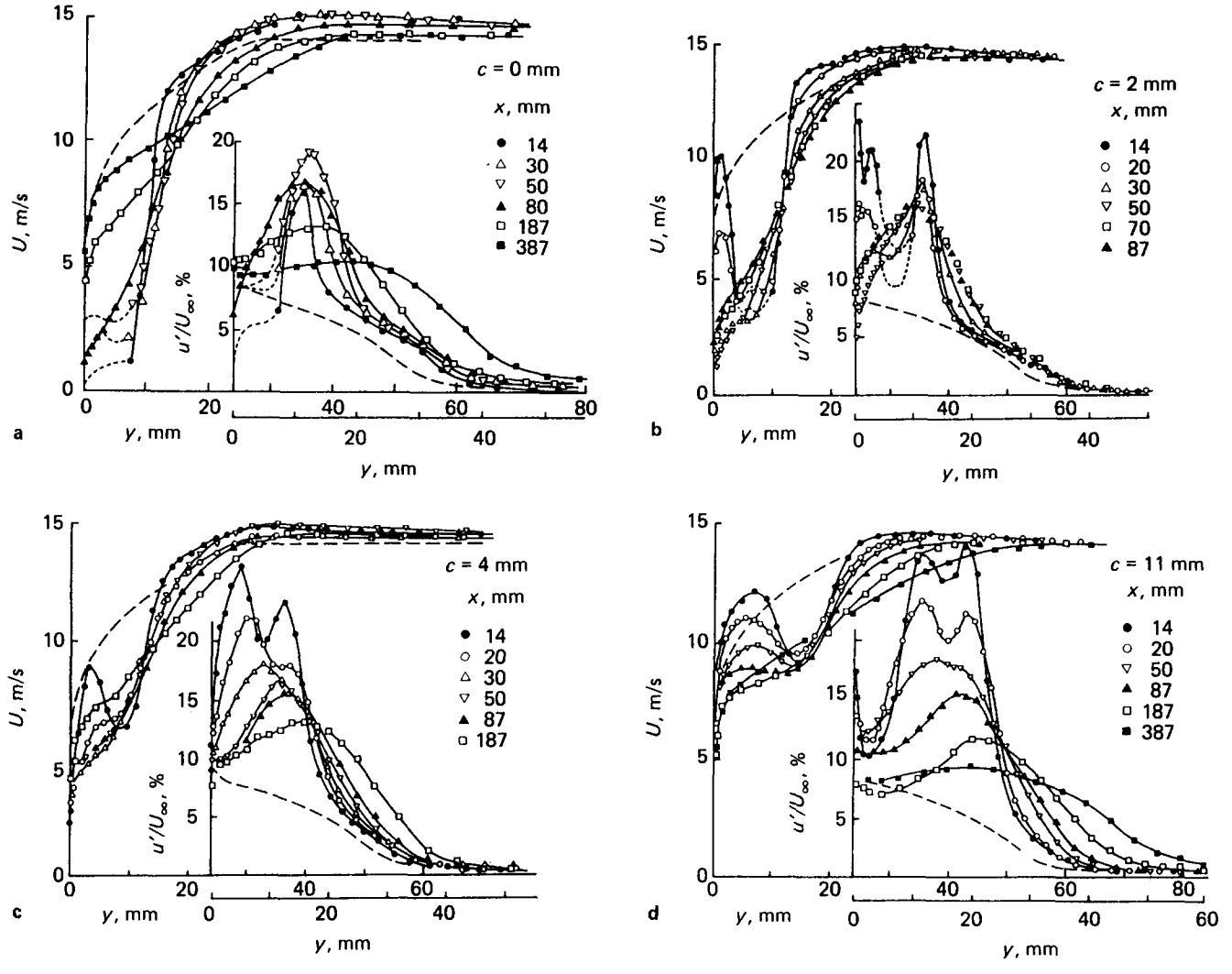

Fig 5 Transverse profiles of mean velocity and fluctuating intensity: (a) c = 0 mm, broken line – undisturbed case; (b) c = 2 mm, broken line – undisturbed case; (c) c = 4 mm, broken line – undisturged case; (d) c = 11 mm, broken line – undisturbed case

wall[11]. Thus the data in Fig 6(a) must be discussed with reservation when C_f is close to zero or negative. In Ref 2, the logarithmic law of the wall was confirmed to hold at positions of $x \geqslant 87$ mm for a case of $c = 2$ mm ($c/d = 0.25$) and at positions of $x \geqslant 37$ mm for two cases of $c = 11$ or 29.5 mm ($c/d = 1.38$ or 3.69). At these positions, the accuracy of the results plotted in Fig 6 is believed to be satisfactory. Figs 7(a) to 7(c) present the streamwise distributions of static pressure measured on the flat plate. In contrast to the static pressure in the main flow, which is uniformly distributed except for a sudden change at the position where the cylinder is located, the wall static pressure varies markedly with streamwise location and the value of c. The value of C_p was evaluated using the following definition:

$$C_p = \frac{p_w - p_\infty}{\frac{1}{2}\rho U_\infty^2} \tag{3}$$

where p_∞ is the static pressure in the main stream measured at a station downstream of the cylinder. The positive asymptotic value of C_p found at a location of $x < -150$ mm corresponds to the magnitude of sudden change of the static pressure in the main flow at the cylinder position.

Case when $c = 0$

As shown in Fig 3(a), when the cylinder is attached to the plate, deterioration of the heat transfer occurs in a region of x just downstream of the cylinder. In the region of $x < 75$ mm, negative values of C_f are found, shown in Fig 6(a), when $c = 0$. It is difficult to determine accurately the exact location of the reversed flow region from the distribution of C_p. However, it is reasonable to assume that the first minimum of C_p which exists around $x = 30$ mm is located at the eye of the recirculating flow. This is because the reversed flow attains its largest streamwise velocity there. It is also reasonable to assume that the flow reattachment point is located at the position where the static pressure at the wall is still increasing as one moves downstream. This is because the transverse distribution of the mean streamwise velocity in the viscous sublayer must be concave in shape; otherwise, the location is certainly bound to be swept by the reversed flow because the velocity gradient at the wall must be zero at the flow reattachment point. The data for C_p obtained for $c = 0$ are noticeably scattered. However, it is reasonable to estimate that the flow reattachment point may be situated at a position of $x < 100$ mm. After $x = 100$ mm the pressure gradient is almost zero. The mean velocity profile

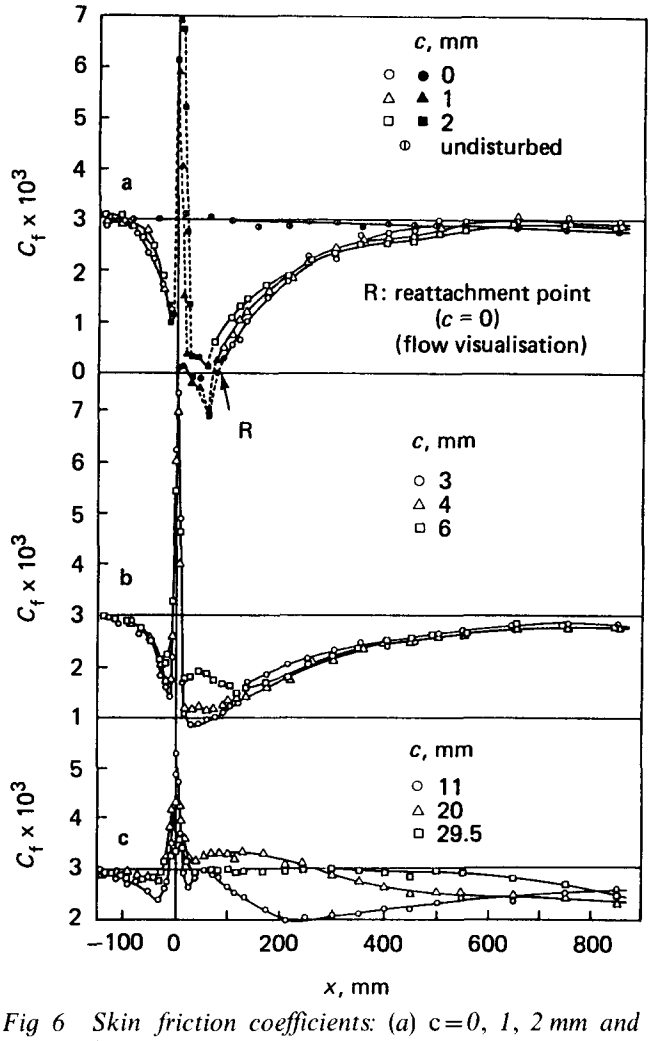

Fig 6 Skin friction coefficients: (a) c=0, 1, 2 mm and undisturbed case; (b) c=3, 4, 6 mm; (c) c=11, 20, 29.5 mm

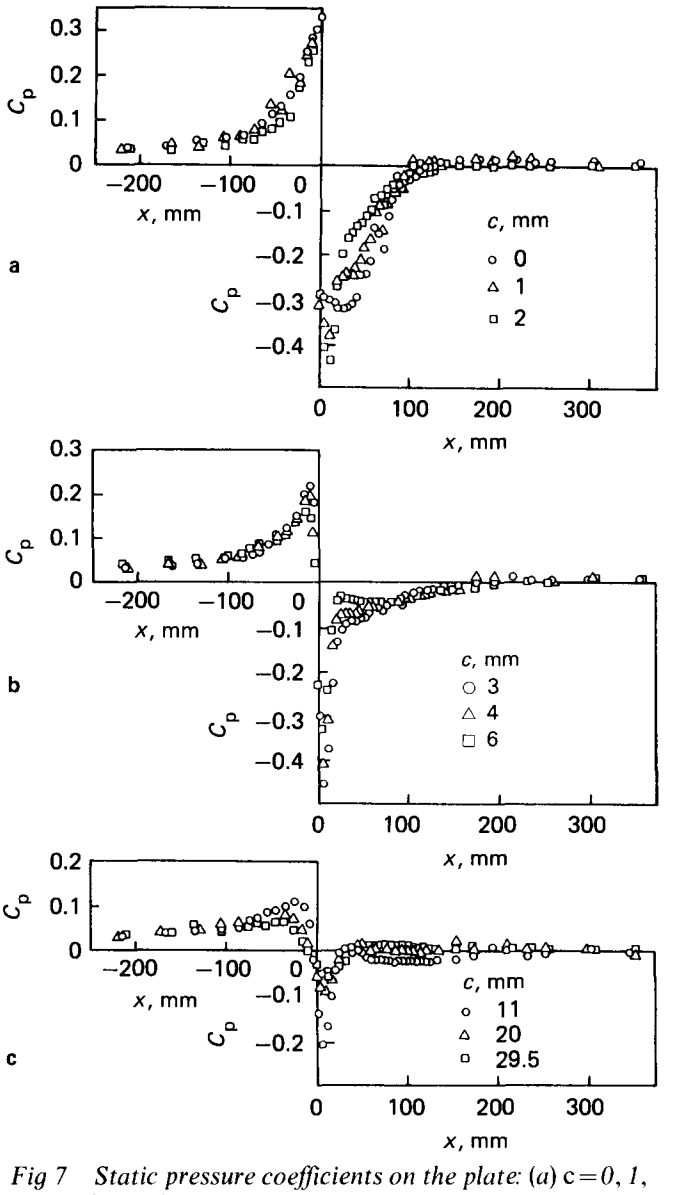

Fig 7 Static pressure coefficients on the plate: (a) c=0, 1, 2 mm; (b) c=3, 4, 6 mm; (c) c=11, 20, 29.5 mm

shown in Fig 5(a) is consistent with this conjecture. The U profile measured at $x=87$ mm already shows a smooth but steep increase with increasing y, and looks unrealistic for a reversed flow region. The streamwise position of the flow reattachment point was also studied from visualization experiments. The results of all three methods mentioned before were found to agree well with each other within experimental accuracy. The position determined was found to agree roughly with the position of $C_f=0$ and is shown in Fig 6(a). Taking these points into consideration, the deterioration of heat transfer is considered to occur in the first half of the flow separation bubble behind the cylinder. The flow has a low velocity there. Additionally, the fluid temperature is rather high in this region because a somewhat large temperature gradient lies in the separation shear layer[2]. These may be the reasons for the deteriorated heat transfer observed there.

The heat transfer is increased when the cylinder is detached from the plate. However, before considering this interesting point, several other features of the h_x distribution obtained when $c=0$ should be noted. The first peak in the h_x distribution found just upstream of the cylinder was still evident even when a small amount of clay was placed around the contact line between the cylinder and the flat plate. Therefore, the condition was not caused by leakage of the fluid through a very small space left beneath the cylinder and the flat plate. A small separation bubble attaching to the front side of the cylinder[13] may have an influence on the peak value of h_x, but it is difficult to comment further on this. More important from the heat transfer technology viewpoint is the second peak of h_x appearing around $x=85$ mm or $x/d=1.05$, where d is the cylinder diameter. This position of peaked heat transfer agrees well with the results obtained by Mori and Daikoku[14] and Edwards and Sheriff[15]. The location of this peak value of h_x corresponds roughly to the flow reattachment point as identified by our earlier discussion. In some axisymmetric recirculating flows, maximum heat transfer has been observed to occur at a position spatially separated from the flow reattachment point[16,17]. It is difficult to judge if this is true in the present flow situation, and it would require a more precise study.

Cases when $c\neq0$

The discussion is now turned to the h_x distributions obtained when $c>0$. When a space is provided between the cylinder and the flat plate, the flow is accelerated

beneath the cylinder and this can cause higher h_x values in this region. This heat transfer enhancement is limited to a small region around $x=0$ as shown in Figs 3(a) to 3(c). Therefore, attention, is paid to other features of the h_x distributions.

When the cylinder is detached from the plate, there is no counterpart of the flow reattachment point existing in the case of $c=0$ in a strict sense. However, when the clearance is small, divergence of the streamlines occurring downstream of the cylinder still ensures a large positive pressure gradient near the flat plate in this region. This is evident in Fig 7 for the two cases of $c=1$ mm and 2 mm ($c/d=0.13$ and 0.25). On the other hand, the static pressure is kept uniform in the main stream as explained before. Thus a large transverse pressure gradient continues to exist in these two cases in the near wall region, as in the case of $c=0$. Thus the upper separation streamline starting from the cylinder surface tends to be inclined toward the flat plate. This is a condition which causes the near-wake flow pattern to be similar to that at $c=0$. In other words, the recirculating flow behind the cylinder sweeps the flat plate more or less in a steady manner in these two cases.

Particularly at the smallest clearance, $c=1$ mm ($c/d=0.13$), the recirculating flow region attaching to the plate may exist behind the cylinder almost in a steady manner. This idea is supported by the negative values of C_f found in Fig 6(a). It also agrees with the flow pattern studied by Bearman and Zdravkovich[18]. While the boundary layer thickness to cylinder diameter ratio differs largely between the present study and Ref 18, the near-wake flow pattern visualized with a smoke method in Ref 18 for small clearance is quite similar to the counterpart for zero clearance. (The value of c/d reported for Fig 6(b) in Ref 18 is 0.2; however, from the photograph, its value appears to be actually 0.1 and, therefore, to correspond roughly to the present case of $c=1$ mm ($c/d=0.13$). A value of half that reported is used for c/d in the following citation.) The flow pattern studied in Ref 18 for $c/d=0.2$ is largely different from that for $c/d=0.1$. Still, periodical shedding of vortex is not reported in the case of $c/d=0.2$. However, in Ref 2, Karman-like vortices were detected at reduced frequency when $c=2$ mm ($c/d=0.25$). Thus, at the clearance $c=2$ mm ($c/d=0.25$), the recirculating flow still sweeps the flat plate in a large time fraction but its unsteadiness becomes larger.

All the above discussion is in accordance with the present flow visualization experiment. A flow reattachment line was actually observed when $c=0$ or 1 mm ($c/d=0$ or 0.13). But when $c=2$ mm ($c/d=0.25$), and at larger value of c, no flow reattachment line was observed. The unsteady or intermittent appearance of the separated flow region causes a sporadic and intensive exchange of momentum and heat between the fluid inside and outside the flow separation bubble. Therefore, the wall heat transfer does not continue to deteriorate significantly downstream of the cylinder. This is one of two possible reasons why improvement in the heat transfer is obtained at a location close to the cylinder when the cylinder is slightly above the plate.

The intensity of the near wall turbulence can sometimes be a governing factor for the wall heat transfer[19]. In Fig 5(b), the transverse distributions of turbulence intensity obtained at the two streamwise locations closest to the cylinder, $x=14$ mm and 20 mm, show higher values near the wall. This may be the direct cause of the enhanced heat transfer responsible for the second h_x peak for the case when $c=2$ mm ($c/d=0.25$). Further support for this idea will be discussed later. This second peak becomes more pronounced when c is further increased to $c=6$ mm ($c/d=0.75$). When $c\geqslant 3$ mm ($c/d\geqslant 0.38$), this peak engulfs the third one. The latter peak is of the same character as the second one which was observed at the flow reattachment point for the case of $c=0$ mm. When $c\geqslant 6$ mm ($c/d\geqslant 0.38$), the second h_x peak completely dominates the heat transfer characteristics downstream of the cylinder.

Since the reliability of the hot-wire data is not high at the two locations $x=14$ mm and 20 mm for $c=2$ mm ($c/d=0.25$), the idea mentioned above for the role of intensive near wall turbulence is discussed from another viewpoint. As seen from the u' profiles plotted in Fig 5(b), the intense turbulence causing the important peak in the h_x distribution must be generated in one of the two shear layers formed across the cylinder wake. In accordance with the spread of the cylinder wake, the intensive turbulence generated in the lower half of the wake is conveyed closer to the plate as the flow goes downstream. The edge of the spreading wake requires a larger streamwise distance to reach the wall region when the space between the cylinder and the plate is larger. It is seen from Fig 3 that the streamwise distance of the second h_x peak from the cylinder, x_{max}, increases with an increase of c. This distance obtained for the cases of $c\leqslant 11$ mm ($c/d\leqslant 1.38$) can be approximated by the following relationship:

$$x_{max}=\frac{1}{1.9^2}\left(c+\frac{d}{2}\right)^2+13.6 \tag{4}$$

This corresponds closely to a theoretical expression obtained from an empirical formula for the spread of the wake of a cylinder located in uniform flow:

$$x_{max}=\frac{1}{\alpha^2}\left(c+\frac{d}{2}\right)^2+\beta \tag{5}$$

The similarity between Eqs (4) and (5) gives further support to the above-mentioned deduction that the second peak of h_x distribution at $c=2$ mm ($c/d=0.25$) and at other larger clearances is caused by the intense near wall turbulence.

As shown in Figs 3(a) to 3(c), the flat plate heat transfer is enhanced to a large degree when the cylinder is slightly raised above the plate compared to the case when it is attached to the plate. From the discussions just completed, it may be concluded that an additional factor influencing the enhanced heat transfer is the intense turbulence which reaches the wall region from the lower shear layer of the cylinder wake. Figs 8(a) and 8(b) show the streamwise distributions of u' measured at $y=4$ mm for the two cases of $c=0$ and 2 mm ($c/d=0$ and 0.25), and the distribution of the local heat transfer coefficient h_x. The u' and h_x distributions are similar in shape at $c=0$ and 2 mm ($c/d=0$ and 0.25). It should be remembered that the measurements of u' are not highly accurate at the positions $x\leqslant 80$ mm in these two cases. However, an interesting point found in this figure is that the flat plate heat transfer is closely related to the intensity of near wall turbulence even at positions far downstream from the cylinder. However, to be fair, it must be pointed out that

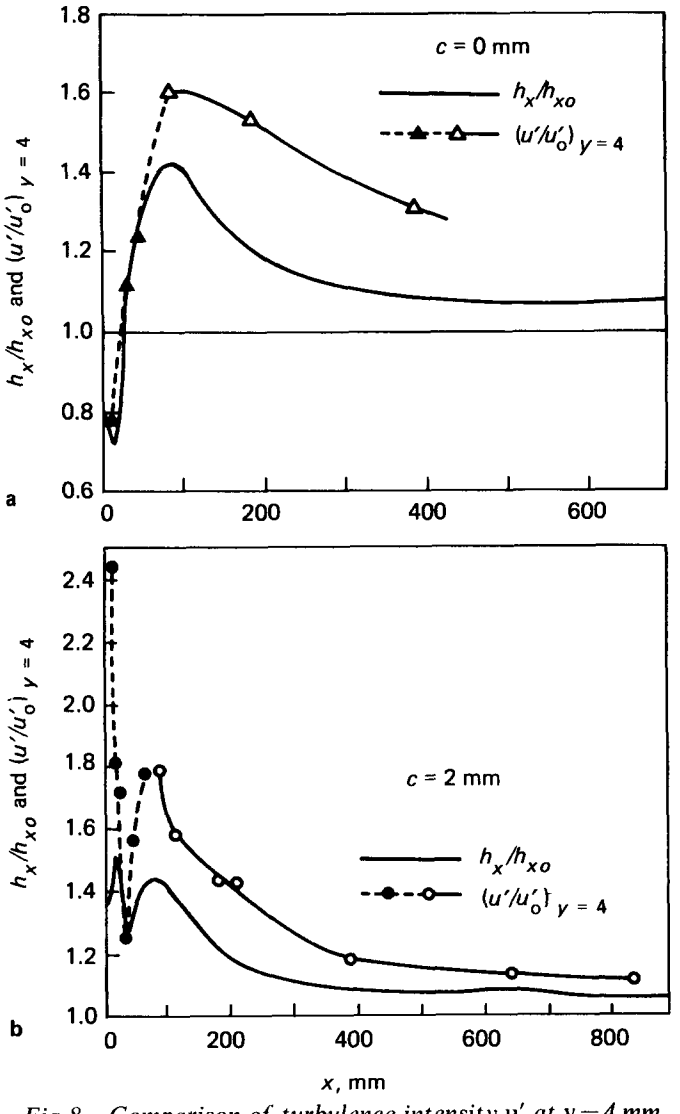

Fig 8 Comparison of turbulence intensity u' *at* y = *4 mm with local heat transfer coefficients: (a)* c = *0 mm; (b)* c = *2 mm*

the intensity of the near wall turbulence is not the sole governing factor of the wall heat transfer. A structural study of the same disturbed boundary layer pointed out that the periodic fluctuation relating to the Karman-like vortex shedding from the cylinder does not play a significant role in triggering the bursting phenomenon[6]. Therefore, when the periodic change of flow contributes significantly to the turbulence intensity, it is not surprising that the turbulent transport of heat and momentum is not dominated by the intense near wall turbulence. While this point must be investigated more carefully in the future, it may partially explain why the value of h_x is not high at the immediate vicinity of the cylinder when $c = 11$ mm ($c/d = 1.38$). This case will be discussed next.

When the cylinder is located at a considerable distance from the plate, no heat transfer augmentation is obtained. Downstream of the cylinder the shear layer turbulence decays or its absolute intensity is reduced. Thus, it is reasonable that the magnitude of the second h_x peak is reduced as the cylinder is moved to $c = 11$, 20 and 29.5 mm ($c/d = 1.38$, 2.5 and 3.69). A second reason for the less effective augmentation of the heat transfer observed when c is increased beyond 11 mm ($c/d = 1.38$) is connected with the disappearance of the third h_x peak which was present at $c < 6$ mm ($c/d < 0.75$). As pointed out above, this peak is created by a flow phenomenon similar to that which created the second peak in the h_x distribution observed when $c = 0$. When the cylinder is detached far enough from the plate, there is no counterpart of the flow reattachment point existing in the case $c = 0$. Thus, the peak caused by this phenomenon becomes less pronounced and finally vanishes at large values of c. Incidentally, less effective augmentation in heat transfer found at large values of c may also be related to the marked contribution of periodical fluctuation to the near wall fluctuation intensity. In Fig 5(d) for instance, the intensity of the near wall turbulence is high at the two locations $x = 14$ mm and 20 mm, but in Fig 3(c) the h_x value is not high at such locations. In Ref 2, periodical shedding of Karman-like vortex was found in cases of $c/d \geqslant 0.25$. This vortex shedding may cause the flow to breathe at the gap between the cylinder and the plate. Thus, in the case of $c = 11$ mm ($c/d = 1.38$), the flow near the wall can fluctuate, even as close to the cylinder as $x = 14$ mm. This is confirmed in Fig 9 in which the auto-correlations of streamwise velocity fluctuation are plotted. This periodical fluctuation may be ineffective in enhancing the wall heat transfer as discussed earlier.

Conclusion

The characteristic features of enhanced heat transfer found in a turbulent boundary layer disturbed by a cylinder have been discussed. Heat transfer deterioration which occurs just downstream of the cylinder when $c = 0$ can be improved by detaching the cylinder slightly from the flat plate. Heat transfer enhancement results from the unsteadiness of the separation bubble and from the effect of intense turbulence arriving at the plate from the shear layer at the lower boundary of the cylinder wake. Heat transfer enhancement due to these effects decreases with increasing streamwise position downstream from the cylinder. Thus, to maintain an effectively enhanced heat transfer over a long surface, cylinders must be placed in an array at an appropriate streamwise pitch. Heat transfer augmentation becomes less effective when c is increased

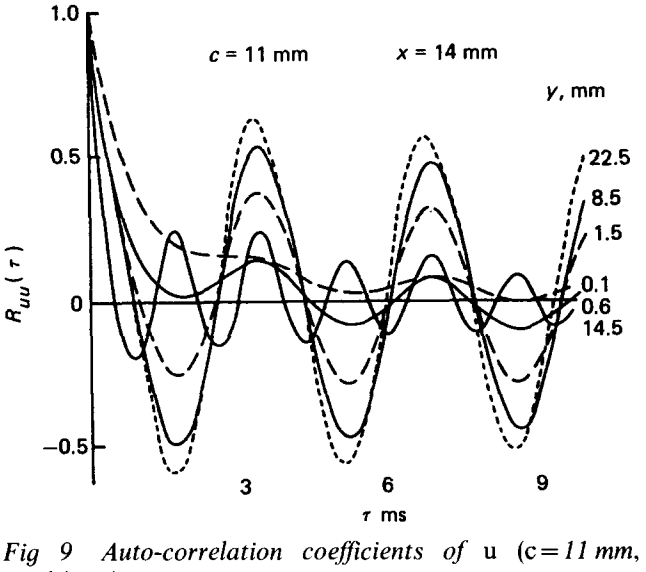

Fig 9 Auto-correlation coefficients of u (c = *11 mm,* x = *14 mm)*

beyond 6 mm ($c/d=0.75$). This is associated with two phenomena. One is related to the fact that the decaying shear layer turbulence requires a longer downstream distance to reach the wall region. The second is related to a reduced tendency for the shear layer formed on the upper side of the cylinder wake to attach to the flat plate when c is increased.

References

1. **Simonich J. C. and Bradshaw P.** Effect of free-stream turbulence on heat transfer through a turbulent boundary layer. *Trans. ASME, J. Heat Transfer, 1978*, **100**, *671*
2. **Marumo E., Suzuki K. and Sato T.** A turbulent boundary layer disturbed by a cylinder. *J. Fluid Mech., 1978*, **87**, *121*
3. **Marumo E., Suzuki K., Sasaki T. and Sato T.** A turbulent boundary layer disturbed by a cylinder located near the wall (1st report, Measurement of one-point double correlation). *Trans. JSME, 1980a*, **46** (*407*), *1211*
4. **Marumo E., Suzuki K., Sasaki T., Kinuta H. and Sato T.** A turbulent boundary layer disturbed by a cylinder located near the wall (2nd report, Production and dissipation rates of turbulent kinetic energy). *Trans. JSME, 1980b*, **46** (*407*), *1220*
5. **Suzuki K. and Kawaguchi Y.** Measurement of bursting period and test of surface renewal model in a turbulent boundary layer disturbed by a cylinder. *Structure of Turbulence in Heat and Mass Transfer* (*ed Z. P. Zarić*) *Hemisphere Publishing Corporation, 1982, 129*
6. **Kawaguchi Y., Yano T. and Suzuki K.** An experimental study on coherent structure in a turbulent boundary layer disturbed by a cylinder. *Proc. 8th Biennial Symp. on Turbulence, Rolla-Missouri, USA, 1983*
7. **Kawaguchi Y., Suzuki K. and Sato T.** Heat transfer promotion with a cylinder array located near the wall. *Int. J. Heat & Fluid Flow, 1985*, **6** (*4*), *249*
8. **Fujita H., Takahama H. and Eki H.** The forced convective heat transfer on a plate with a cylinder inserted in the boundary layer (2nd report, Effects of cylinder diameter and comparison with the case of a square bar). *Trans. JSME, 1981*, **47** (*414*), *317*
9. **Colburn A. P.** A method of correlating forced convection heat transfer data and a comparison with fluid friction. *Trans. AIChE, 1933*, **29**, *174*
10. **Patel V. C.** Calibration of the Preston tube and limitations on its use in pressure gradients. *J. Fluid Mech., 1965*, **23** (*1*), *185*
11. **Nishi M., Imoo Y. and Terazono M.** Measurement of skin friction with improved Preston tube. *Trans. JSME, 1974*, **40** (*331*), *783*
12. **Seki N., Fukusako S. and Hirata T.** Effect of stall length on heat transfer in reattached region behind a double step at entrance to an enlarged flat duct. *Int. J. Heat Mass Transfer, 1976*, **19**, *700*
13. **Kiya M. and Arie M.** Viscous shear flow past small bluff bodies attached to a plane wall. *J. Fluid Mech., 1975*, **69** (*4*), *803*
14. **Mori Y. and Daikoku T.** Study of the influence of two-dimensional roughness on convective heat transfer. *Trans. JSME, 1972*, **38** (*308*), *832*
15. **Edwards F. J. and Sheriff N.** The heat transfer and friction characteristics for forced convection air flow over a particular type of rough surface. *Int. Develop. Heat Transfer, 1961*, **2**, *415*
16. **Kang Y., Nishino J., Suzuki K. and Sato T.** Application of flow and surface temperature visualization techniques to a study of heat transfer in recirculating flow regions. *Flow Visualization II* (*ed Wolfgang Merzkirch*), *1982, Hemisphere Publishing Corporation, 77*
17. **Suzuki K., Kang Y., Sugimoto T. and Sato T.** Circular tube turbulent heat transfer in the downstream of an orifice. *Heat Transfer-Japanese Research, 1982*, **11** (*1*), *70*
18. **Bearman P. W. and Zdravkovich M. M.** Flow around a circular cylinder near a plane boundary. *J. Fluid Mech., 1978*, **89** (*1*), *33*
19. **Suzuki K., Ida S. and Sato T.** Turbulence measurements related to heat transfer in an axisymmetric confined jet with laser doppler anemometer. *Proc. 4th Turbulent Shear Flows, Karlsruhe, FRG, 1983*

Forthcoming articles

Calculation of fin efficiency for condensing fins
S. Achanja, K. G. Brand and A. Attar

Loss and deviation model for a compressor blade element
A. J. Al-Daini

The effects of sound on forced convection over a flat plate
P. I. Cooper, J. C. Sheridan and G. J. Flood

Flow and heat transfer in a rotating cavity with a radial inflow of fluid. 2. Velocity, pressure and heat transfer measurements
M. Firouzian, J. M. Owen, J. R. Pincombe and R. H. Rogers

The importance of turbulence macroscale in determining the drag coefficient of spheres
R. S. Neve

The calculation of turbulent swirling flow through wide angle conical diffusers and the associated dissipative losses
C. B. Okhio, H. P. Horton and the late G. Langer

A Thick Symmetrical Aerofoil oscillating at zero incidence
S. Raghunathan and O. O. Ombaka